# Atom Waves in Crystals of Light

Markus K. Oberthaler, Roland Abfalterer, Stefan Bernet, Jörg Schmiedmayer, and Anton Zeilinger
*Institut für Experimentalphysik, Universität Innsbruck, Technikerstraße 25, A-6020 Innsbruck, Austria*
(Received 23 May 1996)

We present experiments studying the coherent motion of atoms in crystals made from *on* and *off* resonant light. The experiments confirm that inside the light-field atoms fulfilling the Bragg condition form a standing matter wave pattern. As a consequence we observed anomalous transmission of atoms through resonant light fields. [S0031-9007(96)01836-4]

PACS numbers: 03.75.–b, 42.25.–p

Interaction of waves with periodic media provides a plethora of beautiful coherent wave phenomena [1,2] which are particularly striking for deBroglie waves of massive particles. Here we report phenomena of this kind for deBroglie waves of atoms made possible by the recent advent of atom optics [3].

Atoms can easily be manipulated via their interaction with light fields. The enormous advantage is that this interaction can readily be changed by changing the relevant parameters (frequency, power, polarization, momentum distribution) of the light field. Consider a two level atom with an additional strong decay channel of the excited state to a third noninteracting state. The interaction between the light field and the ground state atom can then be described by a complex optical potential [4]

$$V_{\mathrm{opt}}(x,y) = \frac{1}{\hbar}\,\frac{d_e^2 E^2(x,y)}{\Delta + i\gamma/2}\,. \qquad (1)$$

Here $E^2(x,y)$ is the mean square electric field of the light averaged over a light oscillation period, $d_e$ is the electric dipole matrix element of the transition, $\Delta$ represents the difference between the driving light frequency and the eigenfrequency of the transition (detuning), and $\gamma$ is the loss rate from the excited level to the noninteracting state.

It follows from Eq. (1) that one can, besides adjustment of the potential height by changing the light intensity, readily change the potential from effectively real ($|\Delta| \gg \gamma$) to completely imaginary ($\Delta = 0$). A standing light wave therefore mimics a crystal with one set of crystal planes and with arbitrary, real, and complex potential strengths. Generalization to two and three dimensional light crystals and more complex structures is straightforward.

In our experiment, we used Argon atoms in the metastable long-lived $1s_5$ state. This state has a transition (at 801 nm) where the excited state decays predominately (70%) to the ground state. Varying the detuning of an 801 nm standing light wave, we could thus realize any real, complex, or imaginary sinusoidal potential for the metastable Argon atoms. Our detector used can register only the metastable state and therefore atoms pumped to the excited state will escape detection with high probability.

One remarkable phenomenon we experimentally observe is that the total number of metastable atoms transmitted through the standing light wave tuned *on resonance* increases for two specific angles of incidence (see Fig. 1). It turns out that at these angles the atoms fulfill the Bragg condition [5]. Our observation is similar to what Borrmann discovered for x rays in 1941 [6] and what he called *anomalous transmission*.

An interpretation of our observation as Bragg diffraction phenomenon leads to a very satisfying intuitive picture and explanation. Bragg diffraction implies that inside the crystal we obtain two waves, the refracted incident ("forward") wave and the diffracted Bragg wave. These

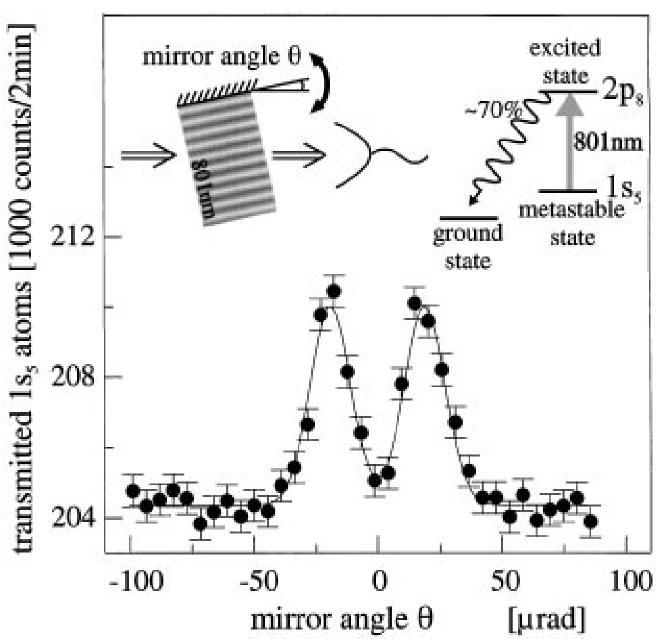


FIG. 1. Total intensity of the metastable Ar* beam after transmission through a standing light wave tuned exactly on resonance to an open transition (see inset) as a function of incidence angle. The transmission increases anomalously for Bragg incidence from either side relative to the planes of the standing light field. The solid line is a fit curve with two Gaussian curves.

 

are coherent with each other and form a *standing atomic wave field*. Its exact location depends on the difference between the wave vectors ($\vec{k}_F$) and ($\vec{k}_B$) of the forward wave and the Bragg diffracted wave and on the phase difference between these two waves. The Bragg condition ($\vec{k}_B = \vec{k}_F + \vec{G}$) implies that the difference between these two atomic wave vectors, $\vec{k}_B$ and $\vec{k}_F$, is equal to the lattice vector $\vec{G}$ which, in turn, is equal to the difference between the two wave vectors $\vec{G} = \vec{k}_{L1} - \vec{k}_{L2}$ (corresponding to a grating period of $\lambda/2$) of the two contributions to the standing light wave. Thus the standing atomic wave field has the same periodicity as the standing light wave and the nodal planes of the two wave fields are parallel.

The transverse position of the atomic wave field with respect to the standing light wave can finally be obtained by applying the principle of extremal interaction found by Horne [7] when investigating the analogous case of neutrons in perfect crystals. Accordingly the eigenstates of the atomic wave field are those exhibiting maximal or minimal interaction. It is clear that the interaction is maximal if the antinodes of the atomic wave field coincide with the planes of maximal light intensity [resulting in the state $\Psi_{\max} = \frac{1}{2}(e^{i\frac{G}{2}x} + e^{-i\frac{G}{2}x}) = \cos(\frac{G}{2}x)$], and it is minimal [$\Psi_{\min} = \frac{1}{2}(e^{i\frac{G}{2}x} - e^{-i\frac{G}{2}x}) = i\sin(\frac{G}{2}x)$] when the antinodes of atomic wave fields are at the nodes of the standing light wave (see Fig. 2). For simplicity of presentation we left out here the longitudinal component of $\vec{k}_{\text{atom}}$. The total wave function is that superposition of $\Psi_{\max}$ and $\Psi_{\min}$ which satisfies the initial boundary condition.

The observed transmission effect of Fig. 1 can thus easily be understood because the rate of depopulation of the metastable state is proportional to the light intensity seen by the atoms and therefore to the overlap between the atom wave field with the standing light field (Fig. 2).

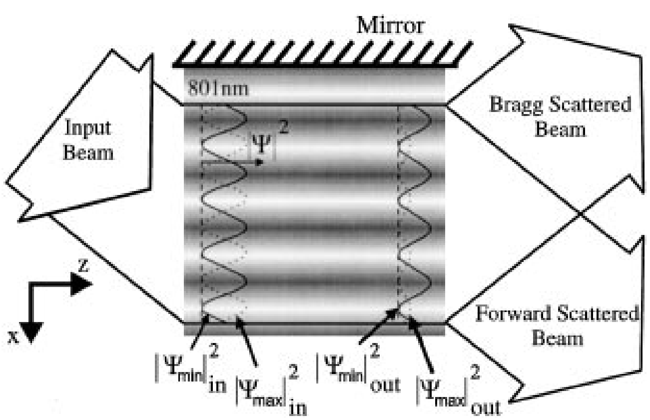


FIG. 2. Standing atomic wave fields for *exact* Bragg incidence inside the standing light field (lower standing light wave intensity represented by darker shading). Initially, the wave field inside the crystal is an equal superposition of $\Psi_{\min}$ and $\Psi_{\max}$ as indicated ($\Psi_{\text{total}}^{\text{in}} = \Psi_{\min} + \Psi_{\max}$). Since the absorption is periodic $\Psi_{\max}$ dies out faster than $\Psi_{\min}$.

The overlap of $\Psi_{\max}$ is much higher than for an off-Bragg plane wave, and thus this wave field is damped out rapidly. On the other hand, $\Psi_{\min}$ has a much lower overlap than an off-Bragg field, and therefore it can survive significantly larger crystal thicknesses. This is the cause of the anomalous transmission effect.

Before presenting the detailed experimental verification of the predictions of our model, we turn to a brief description of our setup.

The metastable Ar beam had an average velocity of 700 m/s ($\lambda_{dB} = 14$ pm). The beam was collimated with two slits better than $\theta_{\text{Bragg}}/2$ with a beam width at the interaction region of $5\mu$m. A movable slit in front of the detector 1,4 m downstream from the interaction region allowed us to measure the far field intensity distribution. That slit was removed for measurements of the total intensity. Further details are given in [8].

The standing light wave was realized using a retro reflecting mirror ($\lambda/10$ flatness) arranged close to the atomic beam inside the vacuum chamber. The planes of stationary phase of the standing light wave and hence the lattice planes of the light crystal are parallel to the mirror surface. Rotating the mirror around a vertical axis results in a change of the angle of incidence of the atoms at the light crystal. The rotation of the mirror using a piezo actuator was calibrated by measuring the tilt angle interferometrically. The accuracy and reproducibility were $\pm 1$ $\mu$rad. The mirror could also be translated in a direction perpendicular to the atom beam with a resolution of 0.5 $\mu$m.

All light beams used originated from commercial laser diodes, passively stabilized using diffraction grating feedback in Littrow geometry and actively stabilized by standard saturation spectroscopy [9]. For the standing light waves, the laser beam was expanded using a Keplerian telescope. The expanded beam was transversely, i.e., in the direction along the atomic beam, limited by an aperture of 4 cm diameter in the experiments measuring the total transmitted intensity (Fig. 1) and of 2.2 cm in the other experiments.

Our model above explains anomalous transmission as a phenomenon arising because of Bragg diffraction of the atomic waves at the light crystal. Thus a Bragg scattered beam is expected behind the standing light wave, even if it is exactly on resonance, i.e., for a purely imaginary potential. In our next experiment, the light crystal was brought into an orientation fulfilling the Bragg condition, and the distribution of atoms in the observation plane was measured by scanning the slit in front of the detector. One indeed observes a Bragg diffracted (B) beam on one side of the straightthrough forward (F) beam and not on the other side.

Within the frame of our model the forward (Bragg) beam is described as a coherent superposition of the amplitudes of $\Psi_{\min}$ and $\Psi_{\max}$ in forward (Bragg) direction. Since $\Psi_{\min}$ and $\Psi_{\max}$ are eigenstates of the Hamiltonian the evolution inside the crystal is given as a superposition of these eigenstates including the phase factor $e^{i\phi(z)}$. Since on resonance the potential is purely complex, $\phi(z)$ is *imaginary*. Straightforward calculation of the overlap integral between the standing light field and the respective standing matter wave field leads to $\phi_{\min}(z) = \frac{1}{4}i\kappa z$ and $\phi_{\max}(z) = \frac{3}{4}i\kappa z$, where $\kappa$ is defined by the evolution of an off-Bragg incident beam $\Psi_{\text{off-Bragg}}(z) = e^{-\frac{1}{2}\kappa z}\Psi_{\text{in}}$. Thus for on-Bragg incidence the intensity of the outgoing beams is given by $|\frac{1}{2}e^{-\frac{1}{4}\kappa z} \pm \frac{1}{2}e^{-\frac{3}{4}\kappa z}|^2 = \frac{1}{4}(e^{-\frac{1}{2}\kappa z} + e^{-\frac{3}{2}\kappa z}) \pm \frac{1}{2}e^{-\kappa z}$, where the plus sign stands for the forward beam and the minus sign for the Bragg beam. For our experiment (Fig. 3) the off-Bragg absorption was $\approx 75\%$, which implies $I_B/I_F = 0.11$. The measured ratio was 0.06. We attribute the difference to factors like the broad velocity distribution of our beam and the different coupling strengths of the magnetic sublevels.

Subsequently the B beam and the F beam were selected separately and the intensities were measured as a function of the angular orientation of the standing light wave mirror. When the slit was positioned such as to allow the F beam to be detected, two peaks did arise again. Even for the direct beam the intensity is higher if the crystal is on-Bragg than off-Bragg. Such a behavior is totally opposite to what one would expect for Bragg diffraction at a nonabsorbing crystal. There, a dip in the forward beam indicates that atoms are diffracted. Only one peak arises (bottom left in Fig. 3), when the detection slit is positioned such as to select the B beam on one side of the forward beam [10]. From a comparison of the measurements of the B beam and the F beam one can deduce that the contribution of the *anomalously* transmitted atoms is equal in both beams.

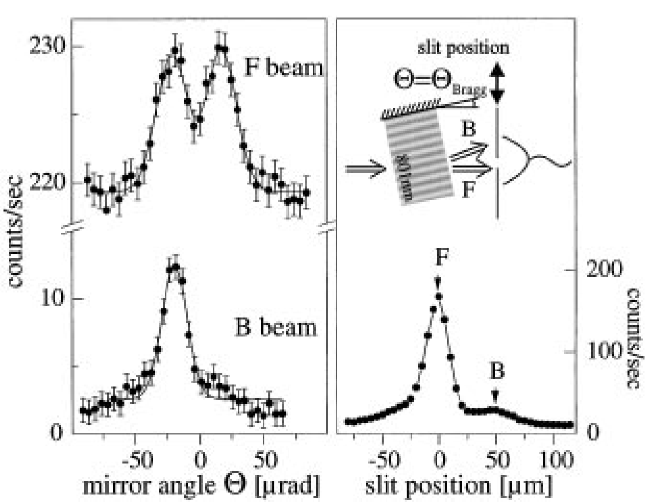


FIG. 3. The right curve shows the far field diffraction pattern for a resonance standing light wave on Bragg. The splitting is the diffraction angle $2\theta_{\text{Bragg}} = 36\mu\text{rad}$. The two curves on the left show the intensities of the forward (F) and Bragg (B) beams (dc background subtracted) as a function of the mirror angle, i.e., the angular orientation of the light crystal [8]. One notices that for Bragg incidence the F beam and the B beam show equal increase of intensity in agreement with our model.

We now turn to observing the atomic wave fields inside the light crystal: Our model implies standing atom wave fields inside the light crystal. Their existence can be seen by the coherence between the B and F beam. The position relative to the crystal is manifested in the phase between B and F beam.

This is demonstrated (Fig. 4) by placing behind the 801 nm light crystal another one with 811 nm light ($1s_5 \rightarrow 2p_9$) tuned far off resonance such that it is not absorptive. There are now two possibilities how an atom can arrive in the B beam: It could have been Bragg diffracted in the first crystal and forward scattered in the second one or forward scattered in the first and Bragg diffracted in the second. Clearly both possibilities have to interfere.

We detected this interference by translating the second crystal with respect to the first crystal along a direction

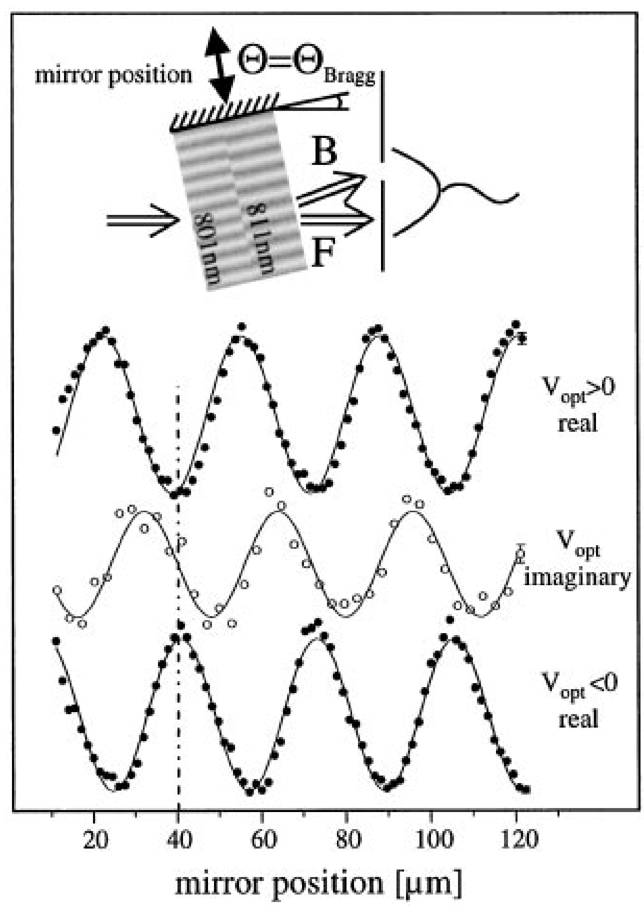


FIG. 4. Measurement of the sinusoidal distribution of the standing atomic wave field. The anomalously transmitted wave field (middle trace) has its maxima at the nodes of the standing light field. If the 801 nm standing wave is detuned off resonance, the standing atomic wave is shifted by $\pi/2$ to the left for blue detuning (positive potential) and to the right for red detuning (negative potential).

transverse to the atomic beam. Because the two crystals have different lattice constants (401 and 406 nm) the relative position of the antinodes in the two standing light waves as seen by the atom could be varied continuously by translating the whole two-crystal assembly. This results in a change of the relative phase between the two interfering atomic beam amplitudes (Bragg-forward and forward-Bragg) and thus finally in a modulation of the intensity of the B beam ($2\pi$ phase shift for 32.4 $\mu$m translation). This is clearly seen in the middle graph of Fig. 4.

Two more sets of data were taken with the 801 nm standing wave also far detuned (not absorptive). In that case, the total atomic wave field inside the crystal is still a superposition of $\Psi_{\rm min}$ and $\Psi_{\rm max}$, that is $\Psi_{\rm total} = \cos(\frac{1}{2}\vec{G}\cdot\vec{x}) + ie^{i\phi(z)}\sin(\frac{1}{2}\vec{G}\cdot\vec{x})$. Compared to the absorptive case $\phi(z)$ is now *real*. The absolute value of $\phi(z)$ is again given by the overlap integral between the optical potential and the corresponding eigenstate.

Calculation shows that, while the relative phase between the B and F beam is $\pi$ for the absorptive crystal, it is $\pm\pi/2$ for a phase crystal, the sign depending on whether the optical potential is positive ($\Delta > 0$, blue detuning) or negative ($\Delta < 0$, red detuning). In other words the resulting total wave function has its maxima at the steepest gradient of the optical potential [Eq. (1)] for a pure phase crystal and has its maxima at the minima of the potential for a pure complex potential.

Experimental observation confirms (Fig. 4) that the intensity oscillations of the B beam are shifted to the left by $\pi/2$ for the blue detuned 801 nm case and to the right by $\pi/2$ for red detuning. The three curves in Fig. 4 clearly demonstrate the existence of the in-crystal standing atomic wave field and show its position relative to the light field.

In conclusion, we want to emphasize that the possibility to build complex light potentials of a wide variety, realizable by diffractive optics and holography, leads to a new tool for creating, manipulating, and investigating matter wave fields. We expect that the experimental possibilities opened up here will lead to detailed and clean investigations of many wave propagation phenomena in periodic media. This will include model systems for similar effects in other areas of physics.

We wish to thank E. M. Rasel and H. Batelaan for many stimulating discussions. This work was supported by the Austrian Science Foundation (FWF), Project No. S06504 and No. P10216, by the U.S. National Science Foundation, Grant No. PHY92-13964, and by of the European Union, Contract No. TMRX-CT96-0002. J. S. is supported by an APART-fellowship of the Austrian Academy of Sciences and S. B. acknowledges an HCM- fellowship of the European Community (Contract No. ERBCHBGCT 940664).

[1] J. M. Cowley, *Diffraction Physics* (North-Holland, Amsterdam, 1990).

[2] The basic framework for the description of diffraction at perfect crystals is the theory of dynamical diffraction closely analogous to the theory of band structures in solids. It treats the wave field inside the periodic structure as a coherent superposition of all scattered wavelets. Overviews for the weak potential limit for photons: B. W. Batterman and H. Cole, Rev. Mod. Phys. **36**, 681 (1964); for neutrons: H. Rauch and D. Petrascheck, in *Neutron Diffraction*, edited by H. Dachs (Springer, Berlin, 1978), p. 303.

[3] A recent overview on atom optics and interferometry is Advances in Atomic, Molecular and Optical Physics: Supplement 3, Atom Interferometry, edited by P. R. Berman (to be published).

[4] D. O. Chudesnikov and V. P. Yakovlev, Laser Phys. **1**, 110 (1991).

[5] Bragg scattering of atoms from a far detuned standing light wave was observed by P. J. Martin, B. G. Oldaker, A. K. Miklich, and D. E. Pritchard, Phys. Rev. Lett. **60**, 515 (1988).

[6] For x rays, see G. Borrmann, Z. Phys. **42**, 157 (1942); for neutrons, see S. Sh. Shilshtein, V. J. Marichkin, M. Kalanov, V. A. Somenkov, and L. A. Sysoev, Zh. Eksp. Teor. Fiz. Pis'ma Red. **12**, 80 (1970); for electrons, see A. Mazel and R. Ayroles, J. Microsc. **7**, 793 (1968).

[7] M. A. Horne, K. D. Finkelstein, C. G. Shull, A. Zeilinger, and H. J. Bernstein, Physica (Amsterdam) **151B**, 189 (1988).

[8] H. Batelaan, S. Bernet, M. K. Oberthaler, E. Rasel, J. Schmiedmayer, and A. Zeilinger, in [3].

[9] One laser diode was tuned to the $1s_5 \rightarrow 2p_8$ transition at 801.7 nm and another one at 795.0 nm served to pump away the parasitic $1s_3$ metastable state (see [8]). A third one served to create 811 nm light for the $1s_5 \rightarrow 2p_8$ transition.

[10] In order to detect the other Bragg diffracted beam corresponding to the second peak of the transmitted beam, one would have to reposition the detector slit symmetrically with respect to the F beam.

[11] One notices that in Fig. 3, the peaks in the rocking curve are wider and the intensity between the two peaks does not go down all the way to the intensity level far off-Bragg as contrasted to Fig. 1. This follows from the increased Bragg acceptance angle (given by $\delta\theta/\theta = 1/N$, where $N$ is the number of crossed lattice planes) for the 2.2 cm wide crystal in Fig. 3 compared to a 4 cm wide crystal in Fig. 1.